

The Critical Coagulation Concentration of Counterions: Spherical Particles in Asymmetric Electrolyte Solutions

JYH-PING HSU¹ AND YUNG-CHIH KUO

Department of Chemical Engineering, National Taiwan University, Taipei, Taiwan 10617, Republic of China

Received June 12, 1996; accepted September 3, 1996

The ratio of the critical coagulation concentration (CCC) of counterions is evaluated for spherical particles and asymmetric electrolytes. A perturbation method is adopted to solve the Poisson–Boltzmann equation governing the electrical potential distribution of the system under consideration. On the basis of the result obtained, an approximate expression for the CCC is derived. Another approach based on the Derjaguin approximation is also used to estimate the CCC. We show that the CCC ratio of counterions is a complicated function of the valences of the ion species in the liquid phase and the sizes of particles. Depending upon the thickness of the Debye length, the CCC ratio of counterions for various combinations of electrolytes can be estimated. The classic Schulze–Hardy rule for planar particles in a symmetric electrolyte solution can be recovered as a limiting case of the present model. If the surface potential is low, the effect of curvature on the CCC ratio of counterions is negligible. © 1997 Academic Press

Key words: critical coagulation concentration, counterions, ratio; particles, charged, spherical; electrolyte solutions, asymmetric; interaction energy, Derjaguin approximation; Poisson–Boltzmann equation, perturbation solution.

INTRODUCTION

The minimum concentration of electrolyte required to induce the coagulation of a stable colloidal suspension is defined as the critical coagulation concentration (CCC). The CCC of counterions is found to be inversely proportional to the sixth power of its valence, the so-called Schulze–Hardy rule. For counterions of valences 3, 2, and 1, this rule suggests that the CCC ratio is $3^{-6}:2^{-6}:1^{-6}$, or roughly, 1:11:729. The Schulze–Hardy rule can be interpreted theoretically by the DLVO theory (1), which considers the electrostatic repulsion force and the van der Waals attraction force between two interacting particles. The key assumptions made in the derivation of this rule are planar surfaces, symmetric electrolytes, and a high level of surface potential (1). Although some of these assumptions are violated obviously (2) and

deviations in the experimental observations from the theoretical predictions are not uncommon (3, 4), the Schulze–Hardy rule is still widely adopted in practice for its convenience.

The difficulty of modifying the Schulze–Hardy rule to a general case depends largely on the types of electrolyte and the shapes of a particle. These factors are closely related to the resolution of the Poisson–Boltzmann equation governing the electrostatic potential distribution around a charged surface (5–9). The solution to this equation is essential to the evaluation of the electrostatic repulsion force between two particles. Since the exact analytical solution to the Poisson–Boltzmann equation under a general condition has not been reported, the corresponding CCC is unknown. In a recent study, an attempt was made to take the asymmetry of electrolytes into account for planar particles. It was found that for a common monovalent anion, the CCC ratio of counterions for valences 3, 2, and 1 is roughly proportional to the -6.35 power of the counterion valence (10).

In the present study, the Schulze–Hardy rule is extended to the case of spherical surfaces in an arbitrary $a:b$ electrolyte solution. In other words, the effect of the curvature of dispersed entities on the CCC ratio of counterions is investigated.

MODELING

The analysis is begun by considering a charged spherical particle immersed in an $a:b$ electrolyte solution. Without loss of generality, we assume that the particle is negatively charged. The electrical potential distribution around the particle is described by the Poisson–Boltzmann equation (9)

$$\frac{d^2\psi}{dX^2} + \frac{2}{X} \frac{d\psi}{dX} = \frac{\exp(b\psi) - \exp(-a\psi)}{a + b} \quad [1]$$

where $\psi = e\phi/(k_B T)$, $X = \kappa r$, $\kappa^2 = e^2 a(a + b)n_a^0/(\epsilon_0 \epsilon_r k_B T)$. Here ϕ is the electrical potential, e denotes the elementary charge, κ is the reciprocal Debye length, ϵ_r and ϵ_0 are the

¹ To whom correspondence should be addressed.

relative permittivity of solution and the permittivity of the vacuum, respectively, n_a^0 is the number concentration of cation in the bulk liquid phase, k_B and T are, respectively, the Boltzmann constant and the absolute temperature, and r is the distance measured from the center of the particle. The boundary conditions associated with Eq. [1] are assumed to be

$$\psi \rightarrow 0 \text{ and } (d\psi/dX) \rightarrow 0 \text{ as } X \rightarrow \infty \quad [1a]$$

$$\psi = \psi_0 \text{ at } X = X_0 \quad [1b]$$

where ψ_0 is the dimensionless surface potential and X_0 is the dimensionless radius of the particle, $X_0 = \kappa r_0$, r_0 being the radius. For a sufficiently large X_0 , an approximate solution to Eq. [1] subject to Eqs. [1a] and [1b] is (11)

$$\psi \cong h_0 + \frac{h_1}{X_0} + \frac{h_2}{X_0^2} \quad [2]$$

where

$$\tanh(ah_0/4) = [\tanh(a\psi_0/4)]\exp[-k_3(X - X_0)] \quad [2a]$$

$$h_1 = [1/(ak_3)] \sinh(ah_0/2) \{ \tanh^2(a\psi_0/4) - \tanh^2(ah_0/4) - 2 \ln[\tanh(a\psi_0/4)/\tanh(ah_0/4)] \}, \quad [2b]$$

$$h_2 = \frac{a}{2k_3} \sinh(ah_0/2) \int_{\psi_0}^{h_0} \frac{1}{\sinh^2(ah_0/2)} \left\{ \frac{ak_3}{4} h_1^2 \sinh(ah_0/2) + \frac{2h_1}{1 + \cosh(ah_0/2)} - \frac{4}{a} [\tanh(ah_0/4)][X(h_0) - X_0] - \frac{4 \tanh^2(ah_0/4) - 8 \ln[\cosh(ah_0/4)]}{ak_3 \sinh(ah_0/2)} \right\} dh_0 \quad [2c]$$

with

$$k_3 = \begin{cases} [(k-2)k_1 + 2k_2]/k, & \text{if } k \leq 4 \\ [2k_1 + (k-2)k_2]/k, & \text{if } k > 4 \end{cases} \quad [2d]$$

$$X(h_0) = \frac{1}{2k_3} \ln \left[\frac{\cosh(ah_0/2) + 1}{\cosh(ah_0/2) - 1} \right] \times \left(\frac{\cosh(a\psi_0/2) - 1}{\cosh(a\psi_0/2) + 1} \right) + X_0 \quad [2e]$$

In these expressions, $k_1 = 2/\{k^{1/2}[(k/2)^{2/(k-2)} - 1]\}$, $k_2 = 2/k^{1/2}$, and $k = 2 + 2b/a$ (7).

The electrostatic free energy F'_{el} , for a charged system can be expressed by (11)

$$F'_{el} = -(\epsilon_0\epsilon_r/2) \int \phi \bar{E} \cdot \bar{n} dA \quad [3]$$

where dA is a differential area, \bar{E} is the strength of electric field, and \bar{n} is the unit outer normal vector. For a system containing K particles Eq. [3] gives

$$F'_{el} = \sum_{n=1}^K \left[(\sigma_n/2) \int_n \left(\sum_{\substack{n'=1 \\ n' \neq n}}^K \phi_{n'} \right) dA_n \right] \quad [4]$$

where the subscripts n and n' denote the n th and the n' th particles, respectively, and σ_n is the surface charge density of the n th particle. Here, we assume that the distance between any two particles is on the order of the Debye length. The electroneutrality requires that

$$\sigma_n = \frac{-1}{4\pi r_{0,n}^2} \int_{r_{0,n}}^{\infty} 4\pi r_n^2 \rho_n dr_n \quad [5]$$

where r_n is the distance measured from the center of the n th particle, $r_{0,n}$ is its radius, and ρ_n is the space charge density for the n th isolated particle. The electrical interaction energy I_{el} can be estimated by

$$I_{el}(\underline{L}) = F'_{el}(\underline{L}) - F'_{el}(\infty) \quad [6]$$

where \underline{L} is the set of distance $L_{n,n'}$, $n, n' = 1, 2, \dots, K$, $n \neq n'$, $L_{n,n}$ being the closest dimensionless surface-to-surface distance between particles n and n' with $L_{n,n'} = L_{n',n}$, and $F'_{el}(\infty)$ is the value of F'_{el} when any pair of particles is infinitely apart. For two interacting particles Eqs. [4] and [6] lead to

$$I_{el}(L) = (\sigma_1/2) \int_1 \phi_2 dA_1 + (\sigma_2/2) \int_2 \phi_1 dA_2 \quad [7]$$

where $L = \kappa L_0$, L_0 being the closest surface-to-surface distance between two particles.

Based on Eqs. [2a]–[2c], if X_0 is sufficiently large, the potential distribution for a large $(X_n - X_{0,n}) = \kappa(r_n - r_{n,0})$ can be approximated by

$$\psi_n \cong (A_n + B_n X_n) \exp(-k_3 X_n) \quad [8]$$

where $\psi_n = e\phi_n/k_B T$, and

$$A_n = \left\{ \frac{8}{a} \left[\tanh\left(\frac{a\psi_{0,n}}{4}\right) \right] + \frac{2}{ak_3 X_{0,n}} \left[\tanh\left(\frac{a\psi_{0,n}}{4}\right) \right]^3 \right\} e^{k_3 X_{0,n}} \quad [8a]$$

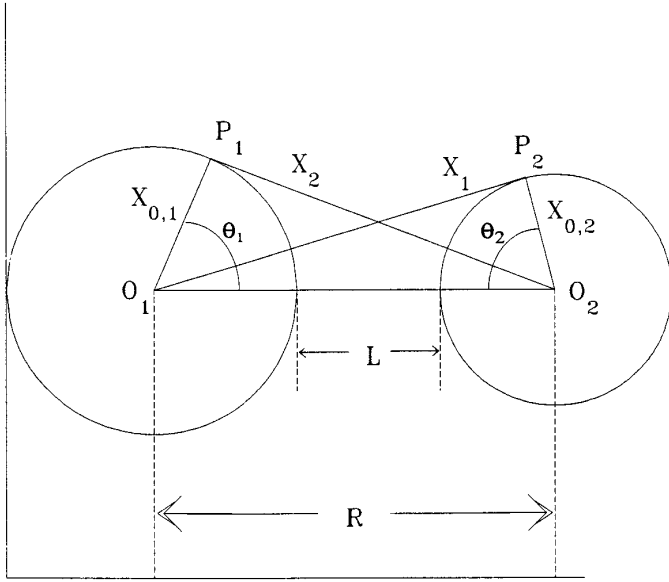


FIG. 1. Schematic representation of two interacting particles. X_1 , X_2 , L , and R are the dimensionless distances; $X_{0,1}$ and $X_{0,2}$ are the dimensionless radii of particles 1 and 2, respectively; θ_1 is the angle defined by the line segments $O_1 - O_2$ and $O_1 - P_1$; and θ_2 is the angle defined by the line segments $O_2 - O_1$ and $O_2 - P_2$.

$$B_n = \left\{ \frac{-4}{aX_{0,n}} \left[\tanh\left(\frac{a\psi_{0,n}}{4}\right) \right] \right\} e^{k_3 X_{0,n}} \quad [8b]$$

By referring to Fig. 1, the differential area dA_n can be expressed as

$$dA_n = 2\pi\kappa^{-2}X_{0,n}^2 \sin \theta_n d\theta_n \quad [9]$$

where θ_n is the angle between line segment $O_1 - O_2(R)$ and $O_n - P_n(X_{0,n})$, R being the dimensionless center-to-center distance between two particles. We have

$$X_{n'}^2 = R^2 + X_{0,n}^2 - 2RX_{0,n} \cos \theta_n, \quad n' \neq n \quad [10]$$

Substituting Eqs. [8]–[10] into Eq. [7] and conducting the integration, we obtain

$$I_{el}(L) \cong \sum_{n=1}^2 G_n(C_n L + D_n) e^{-k_3 L}, \quad n' \neq n \quad [11]$$

where

$$C_{n'} = -4 \left[\tanh\left(\frac{a\psi_{0,n'}}{4}\right) \right] / (aX_{0,n'}) \quad [11a]$$

$$\begin{aligned} D_{n'} = & 2 \left[\tanh\left(\frac{a\psi_{0,n'}}{4}\right) \right] \left\{ \left\{ 4k_3 X_{0,n} \right. \right. \\ & + \left. \left. \left[\tanh\left(\frac{a\psi_{0,n'}}{4}\right) \right]^2 - 4 \right\} / (ak_3 X_{0,n'}) + \frac{4}{a} \right. \\ & + \left. \left\{ -2k_3^2 X_{0,n}^2 + 4k_3 X_{0,n} + (1 - k_3 X_{0,n}) \right. \right. \\ & \times \left. \left. \left[\tanh\left(\frac{a\psi_{0,n'}}{4}\right) \right]^2 - 4 \right\} / [ak_3^2 X_{0,n'}(X_{0,n} + X_{0,n'})] \right. \\ & + \left. 4(1 - k_3 X_{0,n}) / [ak_3(X_{0,n} + X_{0,n'})] \right\} \\ & + C_{n'}(X_{0,n} + X_{0,n'}), \quad n' \neq n \end{aligned} \quad [11b]$$

$$G_n = \pi k_B T X_{0,n} \sigma_{n'} / (ek_3 \kappa^2) \quad [11c]$$

For illustration, we consider two identical particles in the following discussion. In this case, the subscripts n and n' can be dropped.

For a sufficiently small L/X_0 , the van der Waals potential I_{vdw} can be estimated by (1)

$$I_{vdw}(L) = -A_{132} X_0 / 12L \quad [12]$$

where A_{132} is the Hamaker constant. The total interaction energy $I_t(L)$ is the sum of $I_{el}(L)$ and $I_{vdw}(L)$, i.e.,

$$I_t(L) = I_{el}(L) + I_{vdw}(L) \quad [13]$$

At the CCC,

$$I_t = 0 \text{ and } dI_t/dL = 0 \quad [14]$$

Let the value of L at the CCC be L_c . Substituting Eqs. [11]–[13] into Eq. [14], we obtain

$$2G(CL_c + D) \exp(-k_3 L_c) - \frac{A_{132} X_0}{12L_c} = 0 \quad [15a]$$

$$\begin{aligned} & -2k_3 G(CL_c + D) \exp(-k_3 L_c) \\ & + 2GC \exp(-k_3 L_c) + \frac{A_{132} X_0}{12L_c^2} = 0 \end{aligned} \quad [15b]$$

These expressions yield

$$L_c^2 - \left(\frac{2}{k_3} - \frac{D}{C} \right) L_c - \frac{D}{k_3 C} = 0 \quad [16]$$

Since D/C is large for the present system (X_0 is large), we have

$$L_c \cong \frac{1}{k_3} \left\{ 1 - 2 / \left\{ k_3 X_0 + 4 - \left[\tanh\left(\frac{a\psi_0}{4}\right) \right]^2 / 2 \right\} \right\}. \quad [17]$$

If $\psi_0 \rightarrow -\infty$, Eq. [5] leads to (Appendix A)

$$\sigma \propto a n_{a'}^0 / (k_3 \kappa) \quad [18]$$

Substituting Eqs. [17] and [18] into Eq. [15a] yields

$$\frac{n_{a,c}^0}{k_3^3 \kappa^3} \left[\frac{-2}{a} + \frac{3}{ak_3 X_0} - \frac{8}{ak_3 X_0 (k_3 X_0 + 7/2)} \right] \times \left(1 - \frac{2}{k_3 X_0 + 7/2} \right)^2 = \text{constant}, \quad [19]$$

where $n_{a,c}^0$ denotes the CCC of cations (counterions). This expression implies that

$$n_{a,c}^0 \propto \frac{1}{a^3 (a+b)^3 k_3^6} \left[1 - \frac{3}{k_3 X_0} - \frac{8}{k_3 X_0 + 7/2} \left(1 - \frac{1}{k_3 X_0} \right) \right] \quad [20]$$

On the other hand, if $\psi_0 \rightarrow 0$, it can be shown that (Appendix A)

$$\sigma \propto [a(a+b)k_3 e n_a^0 \psi_0 \kappa^{-1}] [1 + (1 + a^2 \psi_0^2 / 32) / k_3 X_0] \quad [21]$$

Substituting Eqs. [17] and [21] into Eq. [15a] yields

$$n_{a,c}^0 \propto \frac{\psi_0^4}{a(a+b)k_3^2} \left[1 - \frac{2}{k_3 X_0} - \frac{8}{k_3 X_0 + 4} \left(1 - \frac{1}{k_3 X_0} \right) \right] \quad [22]$$

Another Approach

If the Derjaguin approximation (12) is applicable, the electrical potential energy between two particles V_{el} can be estimated by

$$V_{el} = \frac{\pi X_0}{\kappa^2} \int_0^{2X_0} \left(1 - \frac{L_1}{2X_0} \right) V_R dL_1 \quad [23]$$

where

$$L_1 = L_2 - L \quad [23a]$$

In these expressions, $L_2 = \kappa L_3$, L_3 is the surface-to-surface

distance between two particles, L is defined under Eq. [7], and V_R is the electrical potential energy for two planar parallel surfaces.

The electrical potential energy V_R can be calculated by (10)

$$V_R = \kappa^{-1} \int_L^\infty F_R dL = \frac{32(a+b)n_a^0 k_B T}{ak_3 \kappa} [\tanh^2(a\psi_0/4)] \exp(-k_3 L) \quad [24]$$

Substituting Eq. [24] into Eq. [23] yields

$$V_{el} = \frac{32(a+b)\pi X_0 n_a^0 k_B T}{ak_3^2 \kappa^3} [\tanh^2(a\psi_0/4)] \exp(-k_3 L_0) \times \left[1 - \frac{1}{2k_3 X_0} (1 - \exp(-2k_3 X_0)) \right] \quad [25]$$

The van der Waals potential, the total interaction energy, and the criterion for CCC are described by Eqs. [12]–[14], respectively. Let L_c be the value of L at which coagulation occurs. Then, Eqs. [12]–[14] and [25] lead to $L_c = 1/k_3$. Substituting this L_c , Eqs. [12] and [25] into Eq. [13], applying Eq. [14], and solving the resultant expression for $n_{a,c}^0$, the CCC of cations, we obtain

$$n_{a,c}^0 = \frac{\lambda \tanh^4(a\psi_0/4) \cdot (4\pi\epsilon_0\epsilon_r)^3 (k_B T)^5 (48)^2}{a^5 (a+b)k_3^6 \cdot e^6 A_{123}^2 \pi (\exp 2)} \quad [26]$$

where

$$\lambda = \left[1 - \frac{1}{2k_3 X_0} (1 - \exp(-2k_3 X_0)) \right]^2 \quad [26a]$$

On the basis of these expressions, the CCC of counterions can be estimated.

If $\psi_0 \rightarrow -\infty$, Eq. [26] gives

$$n_{a,c}^0 \propto \frac{\lambda}{a^5 (a+b)k_3^6} \quad [27]$$

For a sufficiently large X_0 , $\lambda \rightarrow 1$, and Eq. [27] leads to the result for planar particles (10). Furthermore, if the electrolyte is symmetric, $a = b = v$, then

$$n_{a,c}^0 \propto 1/v^6 \quad [27a]$$

This is the Schulze–Hardy rule.

TABLE 1
Variation in the Ratio $[n_{a,c,a:b}^0/n_{a,c,3:3}^0 (X_0 \rightarrow \infty)]$ as a Function of X_0 and the Types of Electrolyte for $\Psi_0 \rightarrow -\infty$

$a:b$	X_0	∞	200	100	80	50	30	20
3:3		1.000	0.945	0.893	0.868	0.793	0.699	0.527
3:2		1.384	1.311	1.241	1.207	1.108	0.941	0.749
3:1		1.522	1.449	1.379	1.345	1.244	1.075	0.880
2:3		7.379	6.964	6.562	6.366	5.798	4.850	3.766
2:2		11.391	10.774	10.177	9.886	9.038	7.622	5.998
2:1		17.232	16.365	15.525	15.113	13.915	11.904	9.586
1:3		276.161	258.242	240.998	232.618	208.382	168.368	123.157
1:2		365.385	343.833	323.022	312.882	283.464	234.590	178.920
1:1		729.000	689.550	651.346	632.691	578.431	487.813	383.888

On the other hand, if $\psi_0 \rightarrow 0$, Eq. [26] leads to

$$n_{a,c}^0 \propto \frac{\lambda}{a(a+b)k_3^6} \tag{28}$$

For a large X_0 this expression becomes the result for planar particles. Furthermore, if $a = b = v$, then

$$n_{a,c}^0 \propto 1/v^2 \tag{28a}$$

This is consistent with the result for planar particles (10).

RESULTS AND DISCUSSION

The variation in the ratio $[n_{a,c,a:b}^0/n_{a,c,3:3}^0 (X_0 \rightarrow \infty)]$ as a function of X_0 and various types of electrolyte for $\psi_0 \rightarrow -\infty$ is shown in Table 1. Note that as $X_0 \rightarrow \infty$, the CCC ratio of cations for symmetric electrolytes is 1:11.391:729, the same as that predicted by the Schulze–Hardy rule.

TABLE 2

Approximate CCC Ratio of Counterions at Various Assumed X_0 Ratios and Types of Electrolyte for $\Psi_0 \rightarrow -\infty$

Approximate X_0 Ratio	Types of electrolyte			
	S	A ₁	A ₂	A ₃
20:50:200	1:17.1:1038	1:15.8:784	1:12.1:459	1:11.0:490
30:80:∞	1:14.8:1090	1:14.1:678	1:10.5:388	1:9.5:413
50:100:∞	1:12.8:919	1:12.5:586	1:9.2:330	1:8.3:348
100:200:∞	1:12.1:816	1:11.9:529	1:8.7:294	1:7.8:309
200:∞:∞	1:12.1:771	1:11.9:503	1:8.7:279	1:7.8:292
∞:∞:∞	1:11.4:729	1:11.3:479	1:8.2:264	1:7.4:276

Note. Type S denotes symmetric electrolytes, the X_0 ratio is $X_{0,3:3}:X_{0,2:2}:X_{0,1:1}$, and the $n_{a,c}$ ratio is $n_{a,c,3:3}:n_{a,c,2:2}:n_{a,c,1:1}$. Type A_b denotes asymmetric electrolytes, the valence of anion is b , the X_0 ratio is $X_{0,3:b}:X_{0,2:b}:X_{0,1:b}$, and the $n_{a,c}$ ratio is $n_{a,c,3:3}:n_{a,c,2:2}:n_{a,c,1:1}$.

According to Eqs. [20] and [22], the CCC of counterions is related to the type of electrolyte ($a:b$), and the dimensionless size of a particle $X_0 (= \kappa r_0)$. For a fixed particle size r_0 , the latter is a function of the Debye length, which is related to the concentrations of ions. This means that the CCC ratio of counterions needs to be determined through an iterative procedure; the algorithm presented in Appendix B is suggested.

Table 2 illustrates the CCC ratio of counterions at several assumed X_0 ratios and types of electrolyte for $\psi_0 \rightarrow -\infty$. The result shown in this table reveals that, depending upon the X_0 ratio, the CCC ratio of counterions can take various values.

The variation in the ratio $[n_{a,c,a:b}^0/n_{a,c,3:3}^0 (X_0 \rightarrow \infty)]$ at two levels of X_0 and various types of electrolyte for the case $\psi_0 \rightarrow 0$ is shown in Table 3, and the corresponding CCC ratio of counterions is illustrated in Table 4. If ψ_0 is low, X_0 is about the same for each type of CCC ratio. As suggested by Table 4, the CCC ratio for spherical particles is close to that for planar particles. In other words, if the surface potential is low, the effect of curvature on the CCC ratio of counterions is negligible.

TABLE 3

Variation in the Ratio $[n_{a,c,a:b}^0/n_{a,c,3:3}^0 (X_0 \rightarrow \infty)]$ as a Function of X_0 and the Types of Electrolyte for $\Psi_0 \rightarrow 0$

$a:b$	X_0	∞	20
3:3		1.000	0.583
3:2		1.114	0.664
3:1		1.150	0.722
2:3		1.947	1.109
2:2		2.250	1.313
2:1		2.583	1.572
1:3		6.512	3.355
1:2		7.149	3.946
1:1		9.000	5.250

TABLE 4
Approximate CCC Ratio of Counterions at Various Assumed X_0 Ratios and Types of Electrolyte for $\Psi_0 \rightarrow 0$

Approximate X_0 ratio	Types of electrolyte			
	S	A_1	A_2	A_3
20:20:20	1:2.25:9.00	1:2.18:7.27	1:1.98:5.94	1:1.90:5.75
$\infty:\infty:\infty$	1:2.25:9.00	1:2.25:7.83	1:2.02:6.42	1:1.95:6.51

Note. The symbols are the same as those used in Table 2.

If $\psi_0 \rightarrow -\infty$ and the electrolyte is symmetric, $a = b = v$, and $k_3 = 1$, Eq. [20] becomes

$$n_{a,c}^0 \propto \frac{1}{v^6} \left[1 - \frac{3}{X_0} - \frac{8}{X_0 + 7/2} \left(1 - \frac{1}{X_0} \right) \right] \quad [29]$$

Furthermore, if $X_0 \rightarrow \infty$, a particle can be treated as a flat surface, Eq. [29] reduces to Eq. [27a].

On the other hand, if $\psi_0 \rightarrow 0$ and the electrolyte is symmetric, Eq. [22] gives

$$n_{a,c}^0 \propto \frac{\psi_0^4}{v^2} \left[1 - \frac{2}{X_0} - \frac{8}{X_0 + 4} \left(1 - \frac{1}{X_0} \right) \right] \quad [30]$$

If $X_0 \rightarrow \infty$, then Eq. [28a] is recovered.

Derjaguin Approximation

The variation in the ratio $[n_{a,c,a:b}/n_{a,c,3:3}(\psi_0 \rightarrow -\infty)]$ for various values of X_0 and types of electrolyte for the case $\psi_0 \rightarrow -\infty$ based on the Derjaguin approximation is shown in Table 5. According to Eqs. [27] and [28], the CCC ratio of counterions is a function of the type of electrolyte and the dimensionless size of particle. The algorithm presented in Appendix B can also be employed.

TABLE 5
Variation in the Ratio $[n_{a,c,a:b}/n_{a,c,3:3}(X_0 \rightarrow \infty)]$ as a Function of X_0 and the Types of Electrolyte Solution Based on the Derjaguin Approximation for $\Psi_0 \rightarrow -\infty$

$a:b$	X_0	∞	65	25	10
3:3		1.000	0.985	0.960	0.903
3:2		0.961	0.947	0.924	0.870
3:1		0.676	0.667	0.653	0.618
2:3		11.529	11.345	11.054	10.361
2:2		11.391	11.216	10.940	10.280
2:1		9.693	9.555	9.336	8.814
1:3		1104.646	1084.296	1052.131	975.757
1:2		822.117	808.369	786.613	734.826
1:1		729.000	717.828	700.132	657.923

TABLE 6
Approximate CCC Ratio of Counterions at Various Assumed X_0 Ratios and the Types of Electrolyte Based on the Derjaguin Approximation for $\Psi_0 \rightarrow -\infty$

Type	X_0 Ratio	10:25: ∞	25:65: ∞	65: ∞ : ∞	∞ : ∞ : ∞
Type S		1:12.1:807	1:11.7:759	1:11.6:740	1:11.4:729
Type A_1		1:15.1:1180	1:14.6:1116	1:14.5:1093	1:14.3:1078
Type A_2		1:12.6:945	1:12.1:890	1:12.0:868	1:11.8:855
Type A_3		1:12.2:1223	1:11.8:1151	1:11.7:1121	1:11.5:1105

Note. The symbols are the same as those used in Table 2.

Table 6 illustrates the CCC ratio of cations at several assumed X_0 ratios and types of electrolyte for $\psi_0 \rightarrow -\infty$. The result shown in this table reveals that the CCC ratio of counterions is a function of the types of electrolyte and the particle size.

The variation in the ratio $[n_{a,c,a:b}/n_{a,c,3:3}(X_0 \rightarrow \infty)]$ at two levels of X_0 and various types of electrolyte for the case $\psi_0 \rightarrow 0$ is shown in Table 7. The CCC ratio of counterions for various X_0 ratios is about the same. The result is

$$n_{a,c,3:3}:n_{a,c,2:2}:n_{a,c,1:1} = 1:2.25:9.0$$

$$n_{a,c,3:1}:n_{a,c,2:1}:n_{a,c,1:1} = 1:2.8:13.2$$

$$n_{a,c,3:2}:n_{a,c,2:2}:n_{a,c,1:2} = 1:2.3:10.5$$

$$n_{a,c,3:1}:n_{a,c,2:1}:n_{a,c,1:1} = 1:2.3:13.5$$

In this case, the CCC ratio for spherical particles is insensitive to curvature, similar to the results of Table 4.

The result based on the Derjaguin approximation is readily applicable to a suspension of spherical particles coated with an ion-penetrable charged membrane. In this case we have

TABLE 7
Variation in the Ratio $[n_{a,c,a:b}/n_{a,c,3:3}(X_0 \rightarrow \infty)]$ as a Function of X_0 and the Types of Electrolyte Based on the Derjaguin Approximation for $\Psi_0 \rightarrow 0$

$a:b$	X_0	∞	10
3:3		1.000	0.903
3:2		0.961	0.870
3:1		0.676	0.618
2:3		2.277	2.047
2:2		2.250	2.031
2:1		1.915	1.741
1:3		13.638	12.046
1:2		10.150	9.072
1:1		9.000	8.123

$$n_{a,c}^0 = \frac{\lambda \tanh^4(a\psi_d/4) \cdot (4\pi\epsilon_0\epsilon_r)^3 (k_B T)^5 (48)^2}{a^5(a+b)k_3^6 e^6 A_{123}^2 \pi (\exp 2)} \quad [31]$$

where ψ_d is the dimensionless potential at the membrane-liquid interface (13, 14). If the potential is high, Eq. [31] leads to Eq. [27]. On the other hand, if the potential is low, Eq. [31] reduces to Eq. [28], in general. Suppose that the fixed charges in a membrane phase arise from the exchange of cations in the liquid phase with the protons of the functional groups in membrane to form a complex, and the subsequent dissociation of this complex. If the binding of the cations with dissociated functional groups is sufficiently strong, and there are enough functional groups, then Eq. [31] reduces to Eq. [28], even if the potential is low (15).

A comparison between Tables 1 and 5, and 3 and 7 reveals that the CCC ratio of counterions obtained on the basis of a perturbation solution of the Poisson–Boltzmann equation and that based on the Derjaguin approximation are different appreciably. Since the derivation of the former is more rigorous than that of the latter, it is more reliable. Nevertheless, the Derjaguin approximation provides a quick estimation for the CCC ratio and can be used as an initial guess for the exact value.

In summary, the classic Schulze–Hardy rule is modified to the case of spherical particles immersed in an asymmetric electrolyte solution. We show that the CCC ratio of counterions is a function of both the valences of ion species and the sizes of the dispersed entities. To determine the CCC ratio of counterions for various combinations of electrolytes at a fixed particle size, the thickness of the Debye length needs to be taken into account. The present analysis provides an efficient method for the estimation of the CCC ratio of counterions.

APPENDIX A

Let n_a and n_b be the number concentrations of cation and anion, respectively. Then

$$\rho = aen_a - ben_b \quad [A1]$$

Substituting this expression into Eq. [5] and employing the Boltzmann distributions for n_a and n_b , we have

$$\sigma = -aen_a^0 \int_{r_0}^{\infty} (e^{-a\psi} - e^{b\psi}) \left(\frac{r}{r_0}\right)^2 dr \quad [A2]$$

Since the amount of coion near a charged surface is limited, we assume that it is negligible in the region $(r_0, r_0 + \delta/\kappa)$, δ being a small number, and Eq. [A2] can be approximated by

$$\sigma = \sigma_u + \sigma_v \quad [A3]$$

where

$$\sigma_u = -aen_a^0 \int_{r_0}^{r_0 + \kappa^{-1}\delta} e^{-a\psi} \left(\frac{r}{r_0}\right)^2 dr \quad [A3a]$$

$$\sigma_v = -a(a+b)en_a^0 \kappa^{-1} \left(\frac{d\psi}{dX}\right) \Big|_{X_0 + \delta} \quad [A3b]$$

Equation [A3b] can be calculated by integrating the Poisson–Boltzmann equation in the region $(r_0 + \delta/\kappa, \infty)$, in which the potential is relatively low (8, 9). Substituting Eqs. [2]–[2c] into Eq. [A3a] and collecting terms of the order X_0 as $\psi_0 \rightarrow -\infty$, we obtain

$$\sigma_u \cong \frac{-2aen_a^0}{k_3\kappa} \left\{ \int_0^{k_3\delta/2} \tanh^2 Z dZ + \frac{2}{k_3 X_0} \int_0^{k_3\delta/2} \tanh^2 Z \times \left[Z - \frac{e^{-2Z}}{1 - e^{-4Z}} (1 - 2Z - e^{-2Z}) \right] dZ \right\} \quad [A4]$$

where

$$Z = k_3(X - X_0)/2 \quad [A4a]$$

If δ is proportional to L_c , $k_3\delta/2$ is roughly a constant. The value of σ_v can be evaluated by substituting Eq. [2]–[2c] into Eq. [A3b]. We have, for $\psi_0 \rightarrow -\infty$,

$$\sigma_v = -4(a+b)en_a^0 \kappa^{-1} \left[k_3 + \left(\frac{3}{2} - k_3\delta\right) / X_0 \right] e^{-k_3\delta} \quad [A5]$$

For a strongly charged surface, the effect of curvature on surface charge density is negligible (8, 9), and $\sigma_u \gg \sigma_v$. We conclude that

$$\sigma \cong \sigma_u \propto an_a^0/k_3\kappa, \text{ as } \psi_0 \rightarrow -\infty \quad [A6]$$

On the other hand, if $\psi_0 \rightarrow 0$, the surface charge density is described by Eq. [A3b] with $\delta = 0$. Since $\tanh(a\psi_0/4) \rightarrow a\psi_0/4$, substituting Eqs. [2]–[2c] into Eq. [A3b] leads to Eq. [21].

APPENDIX B

For a fixed particle size,

$$X_0 \propto \kappa \propto [a(a+b)n_a^0]^{1/2} \quad [B1]$$

On the basis of this expression, the ratio of X_0 for various

combinations of $a:b$ electrolytes can be obtained. For example, the effect of counterions can be summarized as follows:

Type S ratio

$$X_{0,3:3}:X_{0,2:2}:X_{0,1:1} = 1: \left(\frac{4n_{a,c,2:2}^0}{9n_{a,c,3:3}^0} \right)^{1/2} : \left(\frac{n_{a,c,1:1}^0}{9n_{a,c,3:3}^0} \right)^{1/2} \quad [\text{B1a}]$$

Type A_1 ratio

$$X_{0,3:1}:X_{0,2:1}:X_{0,1:1} = 1: \left(\frac{n_{a,c,2:1}^0}{2n_{a,c,3:1}^0} \right)^{1/2} : \left(\frac{n_{a,c,1:1}^0}{6n_{a,c,3:1}^0} \right)^{1/2} \quad [\text{B1b}]$$

Type A_2 ratio

$$X_{0,3:2}:X_{0,2:2}:X_{0,1:2} = 1: \left(\frac{8n_{a,c,2:2}^0}{15n_{a,c,3:2}^0} \right)^{1/2} : \left(\frac{n_{a,c,1:2}^0}{5n_{a,c,3:2}^0} \right)^{1/2} \quad [\text{B1c}]$$

Type A_3 ratio

$$X_{0,3:3}:X_{0,2:3}:X_{0,1:3} = 1: \left(\frac{5n_{a,c,2:3}^0}{9n_{a,c,3:3}^0} \right)^{1/2} : \left(\frac{2n_{a,c,1:3}^0}{9n_{a,c,3:3}^0} \right)^{1/2} \quad [\text{B1d}]$$

In these expressions, $X_{0,a:b}$ is the value of X_0 for an $a:b$ electrolyte, type S stands for symmetric electrolytes, and type A_b , $b = 1, 2, 3$, stands for asymmetric electrolytes with common anion valence b . In general, the CCC ratio of counterions needs to be estimated through an iterative procedure. We suggest the following algorithm:

Step 1. Arbitrarily assume an X_0 ratio.

Step 2. The CCC ratio is calculated by reading values of $n_{a,c,a:b}^0/n_{a,c,3:3}^0$ ($X_0 \rightarrow \infty$) from Table 1 for various $a:b$ combinations. Interpolations and extrapolations may be necessary at this stage.

Step 3. Calculate the X_0 ratio by Eqs. [B1a]–[B1d] and back to step 1.

The iteration procedure is continued until the X_0 ratio converges. The corresponding ratio for $n_{a,c}^0$ is the desired CCC ratio of counterions.

Note that if X_0 is sufficiently large, the entry of Table 1 is a weak function of X_0 . In this case, one iteration of the preceding algorithm yields satisfactory result. As an example for the present theory, we assume

$$X_{0,3:1}:X_{0,2:1}:X_{0,1:1} = 20:50:200 \quad [\text{B2a}]$$

The corresponding entries in Table 1 lead to

$$n_{a,c,3:1}^0:n_{a,c,2:1}^0:n_{a,c,1:1}^0 = 0.618:9.336:729 \quad [\text{B2b}]$$

Substituting these figures into Eq. [B1b] gives

$$X_{0,3:1}:X_{0,2:1}:X_{0,1:1} = 20:56:229 \quad [\text{B2c}]$$

which is close to Eq. [B2a].

As an example for the result derived from the Derjaguin approximation, we assume

$$X_{0,3:1}:X_{0,2:1}:X_{0,1:1} = 10:25:\infty \quad [\text{B3a}]$$

The corresponding entries in Table 5 lead to

$$n_{a,c,3:1}^0:n_{a,c,2:1}^0:n_{a,c,1:1}^0 = 1:15.8:784 \quad [\text{B3b}]$$

Substituting these figures into Eq. [B1b] gives

$$X_{0,3:1}:X_{0,2:1}:X_{0,1:1} = 10:27.48:140.21 \quad [\text{B3c}]$$

which is close to Eq. [B3a].

REFERENCES

- Hunter, R. J., "Foundations of Colloid Science," Vol. I. Oxford University Press, London, 1989.
- Overbeek, J. Th. G., *Pure and Appl. Chem.* **52**, 1151 (1980).
- Wiese, G. R., and Healy, T. W., *Trans. Faraday Soc.* **66**, 490 (1970).
- Matijevic, E., Janauer, G. E., and Kerker, M., *J. Colloid Sci.* **19**, 333 (1964).
- Brenner, S. L., and Roberts, R. E., *J. Phys. Chem.* **77**, 2367 (1973).
- van Aken, G. A., Lekkerkerker, H. N. W., Overbeek, J. Th. G., and de Bruyn, P. L., *J. Phys. Chem.* **94**, 8468 (1990).
- Hsu, J. P., and Kuo, Y. C., *J. Chem. Soc. Faraday Trans.* **89**, 1229 (1993).
- Hsu, J. P., and Kuo, Y. C., *J. Colloid Interface Sci.* **167**, 35 (1994).
- Hsu, J. P., and Kuo, Y. C., *J. Colloid Interface Sci.* **170**, 220 (1995).
- Hsu, J. P., and Kuo, Y. C., *J. Colloid Interface Sci.* **171**, 254 (1995).
- Hsu, J. P., and Kuo, Y. C., *J. Chem. Soc. Faraday Trans.* **91**, 1223 (1995).
- Hiemenz, P. C., "Principles of Colloid and Surface Chemistry." Marcel Dekker, New York, 1977.
- Hsu, J. P., and Kuo, Y. C., *J. Colloid Interface Sci.* **166**, 208 (1994).
- Hsu, J. P., and Kuo, Y. C., *J. Colloid Interface Sci.* **171**, 483 (1995).
- Hsu, J. P., and Kuo, Y. C., *J. Colloid Interface Sci.* **174**, 250 (1995).